RADIATION TRANSPORT ANALYSES FOR DESIGN OPTIMISATION OF THE ITER CORE LIDAR DIAGNOSTIC

R. Pampin[1], M.J. Loughlin[2], M.J. Walsh[1]

(1) EURATOM/UKAEA Fusion Association, Culham Laboratory, Abingdon OX14 3DB, UK
(2) ITER Organisation, Cadarache, 13108 St. Paul-lez-Durance, France
raul.pampin@ukaea.org.uk

Systematic analysis of the radiation fields throughout the ITER core LIDAR diagnostic system were performed to support the design optimisation and assessment process, aiming at achieving the required performance in terms of reliability, occupational safety and interface with neighboring systems. Neutron, photon, nuclear heat and material activation responses were estimated for a variety of configurations, and improved using a combination of analytical "rules of thumb" and numerical computations with the ATTILA™ and FISPACT codes. The neutron flux at the backplate of the port plug was significantly reduced (to ~2x10^7 n/cm^2-s) by fine-tuning the reference geometry of the laser labyrinth, and guidelines were provided for quick estimation of the effect of future design changes. The current design has adequate lifetime of essential optical components, in particular absorption in collection windows below ~1%, and reduced dose to workers during maintenance according to the ALARA principle.

I. INTRODUCTION

The Thomson scattering core LIDAR (light detection and ranging) system, or TSCL, is an essential part of the ITER diagnostic capability, providing plasma temperature and density profiles and benchmark for the results of other systems. The required performance imposes harsh engineering challenges to the overall design, which are magnified by the demanding plasma environment and radiation field. Radiation transport analyses are essential for the performance assessment of diagnostic equipment in such situations. The LIDAR design is at a conceptual stage and evaluation of different options and materials was necessary in order to help establish a solution optimised from many different engineering aspects. Adequate service lifetime of essential optical components (mirrors, windows), and minimum radiation dose to workers during maintenance must be pursued. ITER radiological protection and nuclear interface objectives have to be guaranteed.

I.A. The Thomson scattering core LIDAR system

The TSCL system is located inside ITER equatorial port 10. It is required to measure a plasma (electron) temperature range of 0.5 to 40 keV, and a density range of $3x10^{19}$ to $3x10^{20}$ cm^{-3}, with tight error bands ranging from 5 to 10%. The design of this system started in the 1990s and has undergone several reviews; the starting point of the work presented here is described in Ref. 1. An engineering sketch of the laser ray-tracing and in-port configuration is shown in Fig. 1.

A high energy, short pulse laser (e.g. NdYAG 5 J, 250 ps) is fired from the diagnostic room in the auxiliary building, adjacent to the torus hall; the laser light is guided using mirrors and lenses along the port cell area and through a vacuum window (laser window WL), located in an opening in the bioshield, into the port inter-space area. It travels through the port inter-space confined in a thin steel pipe about 350cm in length, which serves as vacuum boundary. The pipe is attached to a supportive capture mirror holder (CM1 holder) serving as interface between the inter-space and the plug. The light travels along a hole in the holder and in the capture mirror itself (CM1), along a so-called laser labyrinth and into the plasma core. Thompson back-scattered light is collected in CM1, directed down the labyrinth into a second capture mirror, CM2, and finally through another vacuum window (WC) back into the port inter-space. The configuration of the optical path from this point onwards was still open to different options at the time of writing. Regardless of the solution adopted, captured light leaves

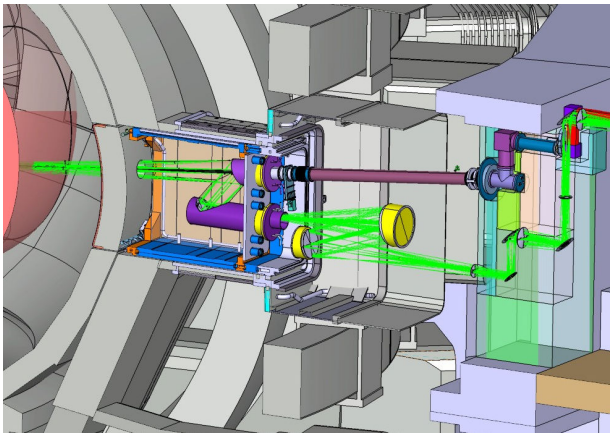

Fig. 1. TSCL core LIDAR system at equatorial port 10.

the bioshield through one or more penetrations and is optically guided back to the diagnostic room for analysis. The port-plug systems (mirrors, mirror holders and laser labyrinth) are housed in a typical ITER diagnostics port plug[2] of dimensions 250 x 215 x 170 cm (L x H x W).

I.B. Constraints and requirements

One of the aims of the radiation transport analyses was to help optimise the system design and integration into ITER by minimising radiation field quantities throughout, but particularly at sensitive locations, whilst maintaining the engineering feasibility and optical performance at desired levels. Several engineering issues were identified as critical for port-plug systems:

(a) position of CM1: the initial position of this mirror, nearly at the back of the plug, maximises lifetime by minimising plasma sputtering and dust deposition;

(b) optical path: the angles between mirrors in the laser path should be kept as low as possible, as aberration is intensified as these angles increase;

(c) CM holders: these provide another engineering challenge; their feasibility and stability are of paramount importance for the overall operability of the system.

In addition, the analysis should support the achievement of the main radiological requirements, which are: to keep absorption in windows as low as reasonably achievable, and in particular below ~1%; to keep dose to personnel 14 days after shutdown as low as reasonably achievable and below 100 μSv/h in the port inter-space area; to keep helium production in adjacent modules of the vacuum vessel below 1 appm, to allow for reweldability of this component; to keep several radiological parameters in neighbouring superconducting coils below their engineering constraints (heat deposition in copper below 1 mW/cc, fast neutron fluence to Nb_3Sn below 10^{18} n/cm^2 per fpy); and to obtain the nuclear heat deposition distribution throughout the systems to enable the provision of a suitable cooling scheme.

II. CALCULATION METHOD

The ATTILA™ discrete ordinates S_nP_ℓ radiation transport code was used for all the calculations reported here, coupled to un-weighted, collapsed versions of the 175-neutron and 42-gamma energy groups (175n42g), FENDL 2.1 fusion reference library. The level of detail differed according to availability of computer resources and requirements of the design process. A high-resolution biased quadrature set was used in all cases to minimize ray effects through the penetration. Irradiation modelled a typical ITER plasma (R_o = 6.2 m, a = 2.0 m, T_{ion} = 20 keV, elongation = 1.7, triangularity = 0.3, peaking factor = 2) normalised to a FW equatorial outboard wall load of 3.45x10^{13} n/cm^2-s, i.e. 0.78 MW/m^2 of mono-energetic 14.1 MeV neutrons[3]. For scoping calculations this was simulated using an anisotropic angular boundary source (hereinafter "boundary source")[4]. For the integration analyses of the latest design, a 3D contour representation of the above plasma was used ("3D source"). The geometry models are described in following sections; all of them assumed ITER-grade stainless steel structures (mirrors, mirror holders, port plug box). The blanket was a mixture of steel, water, copper and beryllium. The port plug shield was assumed to be 50/50vol steel and water.

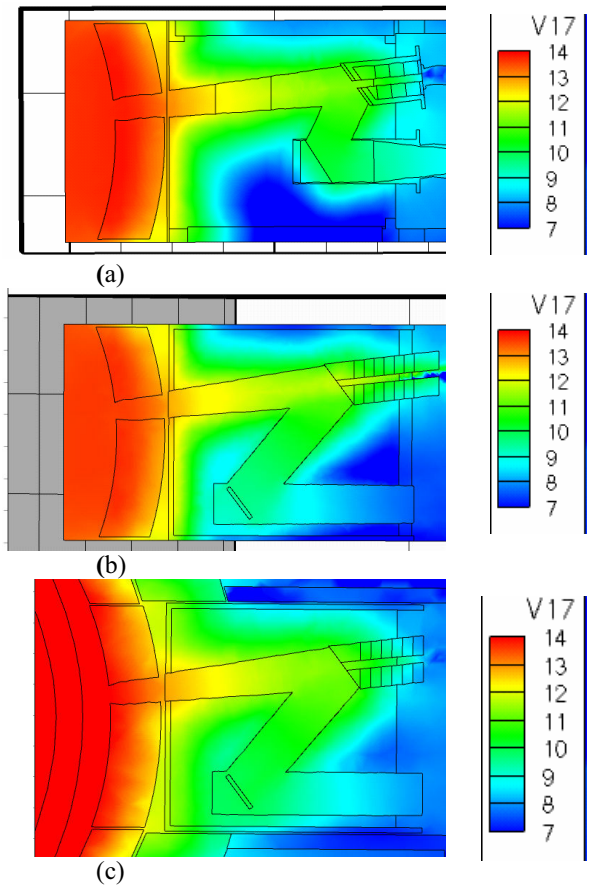

Fig. 2 (color in electronic version). Log of neutron flux (n/cm^2-s) throughout the systems for: (a) reference model, boundary source, (b) optimised model, boundary source, and (c) integrated optimised model, 3D source.

III. PORT-PLUG SYSTEMS OPTIMISATION

III.A. Reference design

Little design margin existed a priori in the port-plug systems area due to the already fine tuning of the optics. A first exploration of the neutron response of the reference design using ATTILA (140,000 elements, P_3, 20n42g), however, revealed that the CM1 holder and WC areas of the backplate presented flux levels which may compromise the ITER zoning compliance of the port

inter-space (Fig. 2a). Exploration of mild variations of the initial configuration was made to ascertain the potential to reduce these levels without compromising the performance and feasibility of the optical equipment.

III.B. Analytical Z-shaped dogleg

The shape of the LIDAR port-plug systems configuration is known as a dogleg penetration. Doglegs are widely used in shielding design as they provide avoidance of direct lines of sight from the radiation source when a penetration of the shield is required for access. The LIDAR dogleg is Z-shaped to optimise the optical performance and reduce aberration.

An approximate analytical solution to the Boltzmann transport equation can be obtained which provides insight into the characteristics of neutron transport in this problem. The flux at the backplate can be approximated by three contributions according to the diagram in Fig. 3: ϕ_1 is the flux component through the upper leg of the laser path, ϕ_2 is the flux through the lower leg of the laser path, and ϕ_3 is the flux scattered in CM1 along the laser labyrinth, down the vertical middle leg and then in CM2 to the backplate. Assuming a uniform, parallel flux source at the first wall surface, ϕ_0, basic solution of the Boltzmann transport equation yields:

$$\phi_1 = \phi_0 e^{-(1-x)/\lambda} \quad (1)$$

$$\phi_2 = \phi_0 e^{-(x-d\tan\theta)/\lambda} \quad (2)$$

$$\phi_3 = \phi_0 \eta_1 \eta_2 \frac{a_2 \cos^2\theta}{4\pi d^2} \frac{a_3}{4\pi(1-x+d\tan\theta)^2} \quad (3)$$

where x is the position of the dogleg bend from FW, λ the mean free path through the shield, θ the angle of the middle leg with the vertical, d the vertical distance between the upper and lower sections, a_i cross sectional areas of each of the sections and η_i neutron albedo of the mirrors; x, d and λ are relative values, normalised to the total length, D. Finally, the average flux at the backplate can be obtained by a weighted sum of these three components:

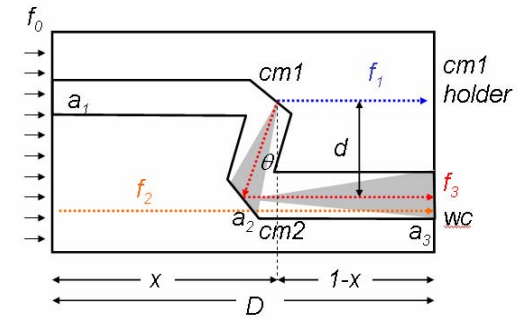

Fig. 3. Diagram of the analytical approximation to the neutron field through a Z-shaped dogleg penetration.

$$\phi_{tot} = (a_1\phi_1 + a_2\phi_2 + a_3\phi_3)/A \quad (4)$$

where A is the total surface area of the backplate. Fig. 4 is a plot of the dependence of these components on the bend position for the following parameters: a_1 = 450 cm^2, a_2 = 1900 cm^2, a_3 = 1000 cm^2, θ =0°, $\eta_1 = \eta_2$ = 0.95, λ·D = 6 cm, d·D = 80 cm, A = 40,000 cm^2, D = 300 cm. These theoretical considerations were tested by parametric modeling with ATTILA. A simple CAD model of the system based on Fig. 2 and the above values was set up which allowed rapid calculations varying all parameters involved, namely x, θ and d. The mesh consisted of ~100,000 elements; $S_{16}P_3$, 20n and TCL quadrature were used in all cases. Parallel irradiation with 14.1 MeV neutrons at the front of the model was considered. Results are compared with the prediction in Fig. 4.

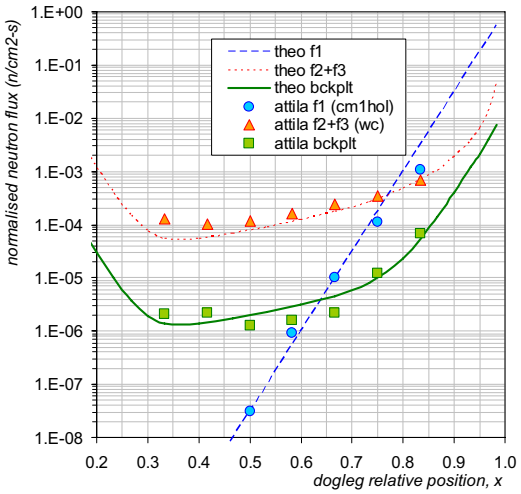

Fig.4. Diagram of analytical approximation to the neutron field through a Z-shaped dogleg penetration (f = ϕ).

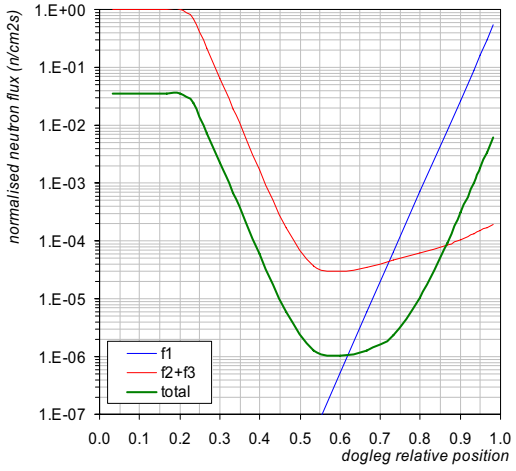

Fig. 5. Analytical approximation to the neutron field through a Z-shaped dogleg penetration for LIDAR (f = ϕ).

Fig. 5 shows the dependence of these three components on the bend position for the actual values of the geometry in the LIDAR system: a_1 = 450 cm^2, a_2 = 1500 cm^2, a_3 = 1400 cm^2, $\theta = 40^o$, $\eta_1 = \eta_2 = 0.95$, $\lambda \cdot D = 6$ cm, $d \cdot D = 80$ cm, A = 40,000 cm^2, D = 300 cm. It appears that the dogleg bend relative position in the reference design at 0.85 (i.e. 250cm from FW) is far from its optimum at about 0.60 (175cm). Moving CM1 to such position would entail unreasonable engineering challenges: severely increased sputtering and more difficult engineering of the mirror holder. Instead, a compromise could be reached by moving the mirror only slightly forward: 25cm (to 0.75) could alleviate ϕ_1 by one order of magnitude (Fig. 5). The lower section and scattering flux components, ϕ_2 and ϕ_3, would remain largely unaffected by this change. To reduce them, use could be made of one of the few remaining flexible parameters in the system: the vertical length. An increase of 50%, from 80 to 120cm, could reduce by an order of magnitude the scattering component whilst not affecting ϕ_3, according to Eqs. (2) and (3).

III.C. Analysis of optimised design

The work described above was input to the design process, and as a result the lay-out of the port-plug systems was updated. A CAD model of the optimised system for ATTILA was prepared and analysed using the boundary source (145,000 elements, P_3, TCL, 20n42g). Fig. 2b shows the neutron field distribution at a vertical slice through the system, in log of the flux. Backplate values matched closely those expected following the analytical analysis presented in previous sections. Indeed, the new in-port configuration (x = 225 cm, d = 120 cm) does appear to result in one order of magnitude less flux at CM1 holder and WC positions. The average flux at the backplate drops by the same amount.

Finally, the optimised model was integrated into an ATTILA-ready version of the so-called "benchmark" 40-degree sector model of ITER[9]. The integrated model was successfully meshed and run using the 3D source (498,000 elements, P_2, 14n14g, TCL). Results are shown and compared with earlier analyses in Figs. 2c and 6; a few, localised negative fluxes were obtained which should not compromise the general validity of the solution. Table 1 summarises the ATTILA results; note that WL fluxes were obtained using the last collided flux approximation.

IV. RESPONSE OF CRITICAL COMPONENTS

Flux levels of the optimised configuration were used to calculate radiological quantities in sensitive components. Of particular interest is the absorption (change in optical thickness) of the window material (fused silica, SiO_2); the following formula describes the change in absorption due to change in optical density by radiation energy deposition:

$$A = 1 - e^{-\alpha . a . \phi . t} \quad (5)$$

where A is light absorption fraction, ϕ neutron flux, t irradiation time, α optical thickness change rate (0.025 cm^{-1}MGy^{-1}), and a a deposition coefficient whose value in the literature ranges from 5 to 320x10^{10} cm^{-2}Gy^{-1}, depending on the neutron spectrum[5,6]. Assuming a relatively moderated spectrum at WC, optimised total flux values give a ~70 fpy lifetime before absorption reaches 1%. Even allowing for a purely fast (14.1 MeV) neutron flux a lifetime of ~11 fpy is obtained. For WL it is reasonable to assume a purely fast flux, it being in direct line-of-sight with the plasma; neutron flux results yield a lifetime of ~0.3 fpy.

Transmutation calculations using the FISPACT inventory code and EAF data libraries[7,8] revealed levels of activation and related quantities at points of interest, namely CM1 and CM1 holder. Typical ITER operation was assumed (3,000 x 400 s pulses per year). Table 1 shows peak activation dose values for CM1 and CM1 holder at the interface with the port inter-space area, based on the contact dose approximation. Design guideline is 100 μSv/h in the port inter-space area.

TABLE I: ATTILA results summary.

model	Ref. 1	reference	optimised	optimised (integ.)	target
source (R_o = 6.2 m, a = 2.0 m, peaking = 2)	Ref. 1	boundary	boundary	3D contour	
CM1 flux (n/cm^2-s)	7x10^{11}	3x10^{11}	5x10^{11}	4x10^{11}	
CM2 flux (n/cm^2-s)	4x10^9	1x10^{10}	6x10^9	7x10^9	
WC flux (n/cm^2-s)	~10^8	2x10^9	5x10^7	3x10^8	
WL flux (n/cm^2-s)	~10^{10}	2x10^9	2x10^9	2x10^9	
backplate average flux (n/cm^2-s)		1x10^8	2x10^7	2x10^7	
CM1 nuclear heat (W/cc)	0.017	0.018	0.021	0.015	
WC lifetime for absorption < 1% (fpy)				11—70	
WL lifetime for absorption < 1% (fpy)				0.3	
CM1 holder peak 14-days activation dose (μSv/hr)		3750	625	800	< 100
peak nuclear heat in Cu at TF coils (mW/cc)				0.02	< 1
peak fast fluence in SC at TF coils (n/cm^2 per fpy)				1x10^{16}	< 10^{18}

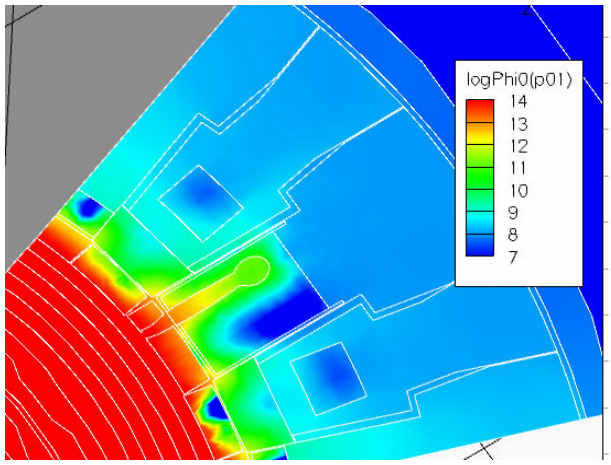

Fig. 6 (color in electronic version). Neutron flux (log of n/cm^2-s) distribution at laser labyrinth upper section level of TSCL (integrated optimised model, 3D source).

V. EFFECTS ON NEIGHBOURING SYSTEMS

The effect of the TSCL penetration in the neighbouring vessel and TF coil was also investigated, and is illustrated in Fig. 6. Peak nuclear heat value in Cu at this vertical level is found to be 0.02 mW/cc, whereas fast (>0.1 MeV) neutron fluence is 1x10^{16} n/cm^2 per fpy. For comparison purposes, a calculation without the LIDAR laser labyrinth penetration was also performed (i.e. solid port plug throughout); a peak nuclear heat value in Cu of 0.009 mW/cc and a fast fluence of 2x10^{15} n/cm^2 per fpy were obtained in this case. Design limits are 1 mW/cc and 10^{18} n/cm^2 per fpy, respectively.

VI. CONCLUSIONS

Systematic analyses of the radiation field throughout the ITER core LIDAR diagnostic systems were performed to assist in the design and integration of the system. Neutron and photon responses were estimated and optimised using a combination of analytical "rules of thumb" and numerical computations using the ATTILA code. Radiation fields throughout the port-plug systems have been minimised within engineering constraints; guidelines are provided to quickly evaluate the effect of future design changes. The optimised design achieves an average flux at the backplate of ~2x10^7 n/cm^2-s (down from ~1 10^8 n/cm^2-s in the reference design), peak 14-day contact dose at CM1 holder of 800 μSv/h after a 3,000 pulse irradiation (down from ~4,000 μSv/h) and, in the neighbouring coils, Cu peak nuclear heat rates of 0.02 mW/cc and fast neutron fluence of 3x10^{15} n/cm^2 per fpy. The estimated response of optical components seems to be within service requirements.

Small uncertainties may have been introduced by the use of un-weighted, collapsed energy groups in some of the analyses; reported values are given to one significant figure only. Their validity is subject to the provision of shielding in the way assumed: solid port plug filled with an homogeneous 50/50 steel water mix. As shown in Table 1, they compare within reason with earlier analyses[1], when accounting for the large differences in materials and geometry lay-out; in particular for CM1 and laser labyrinth.

Future work will be to assist further design reviews, to implement the LIDAR system in the latest reference ITER model "A-lite"[10], in order to confirm the results presented here, to assist in the design and optimization of the bioshield beam dump using numerical calculations and the analytical approximation previously described, and to accurately map the activation dose field in the port inter-space and port cell areas using the rigorous-two-step method with high spatial resolution, in order to overcome the results of the simplistic and over-conservative FISPACT contact dose approximation.

ACKNOWLEDGMENTS

The authors wish to thank Dr. P.H. Morgan (UKAEA Fusion) for his valuable input. This work was funded jointly by the UK Engineering and Physical Science Research Council and the European Communities, under the Contract of Association between EURATOM and UKAEA. The views and opinions expressed herein do not necessarily reflect those of the European Commission.

REFERENCES

1. M. J. WALSH et al., *Review of Scientific Instruments* **31** (2006), p1000.
2. N.H. BALSHAW et al., *Fusion Science and Technology*, this conference.
3. H. IIDA et al., "ITER Nuclear Analysis Report", ITER IDM documentation, ITER_D_22JNMY v1 0.1, July 2004.
4. M.J. LOUGHLIN, R. PAMPIN et al., "Recent developments in neutronics", *Fusion Engineering and Design* (2008), in press.
5. A. IIDA et al., *Transactions in Nuclear Science* **35** (1988), p998.
6. A. RAMSEY et al., *Review of Scientific Instruments* **66** (1995), p1002.
7. R.A. FORREST et al., "FISPACT user manual", UKAEA report **FUS 534**, March 2007.
8. R.A. FORREST et al., "The EAF activation file: neutron-induced reaction cross-sections", UKAEA report FUS 535, March 2007.
9. P.P.H. WILSON, et al., *Fusion Engineering and Design* **83** (2008), p824. doi:10.1016/j.fusengdes.2008.05.038
10. M.J. LOUGHLIN et al., *Fusion Science and Technology*, this conference.